Research Square

Preprints are preliminary reports that have not undergone peer review.
They should not be considered conclusive, used to inform clinical practice,
or referenced by the media as validated information.

CCRL2 deficiency inhibits thermogenesis in mice by altering macrophage polarization

Min Xu
Department of Laboratory Medicine, Northern Jiangsu People's Hospital
Wanqing Li
Department of Center for Clinical Molecular Medicine, Children’s Hospital of Chongqing Medical University, National Clinical Research Center for Children and Adolescents' Health and Diseases
Lin Yuan
Department of Laboratory Medicine, Northern Jiangsu People's Hospital
Xu Lian
17306294517@yzu.edu.cn

Department of Laboratory Medicine, Northern Jiangsu People's Hospital

Article

Keywords: C-C motif chemokine receptor-like 2, macrophage polarization, fat browning, thermogenesis, obesity

Posted Date: March 26th, 2026

DOI: https://doi.org/10.21203/rs.3.rs-8958895/v1

License: This work is licensed under a Creative Commons Attribution 4.0 International License. Read Full License

Additional Declarations: No competing interests reported.

Abstract

Obesity is a global health challenge driven by excessive fat accumulation and disrupted energy homeostasis. While white adipose tissue (WAT) stores energy, brown adipose tissue (BAT) and beige fat mediate thermogenesis. Enhancing WAT browning is a promising anti-obesity strategy. In this study, we demonstrate that C-C motif chemokine receptor-like 2 (CCRL2) deficiency promotes macrophage polarization toward a pro-inflammatory M1 phenotype. This shift inhibits the cyclic adenosine monophosphate (cAMP)-protein kinase A (PKA) thermogenic signaling axis in subcutaneous WAT (sWAT), subsequently suppressing uncoupling protein 1 (UCP1) expression and browning capacity. Notably, this thermogenic impairment occurs independently of the classical β-adrenergic receptor pathway. Interestingly, we observed elevated p38 MAPK phosphorylation despite reduced thermogenesis, suggesting a novel non-adrenergic regulatory mechanism driven by macrophage-adipocyte crosstalk. Our findings identify CCRL2 as a critical immune checkpoint regulating adipose tissue thermogenesis and suggest it as a potential therapeutic target for obesity and related metabolic disorders.

Introduction

Obesity has become a major public health and economic problem because it increases the risk of type 2 diabetes, non-alcoholic fatty liver disease, and cardiovascular and cerebrovascular disorders[1–4]. Obesity thus results from a sustained imbalance between energy intake and energy expenditure that leads to excess energy storage and increased adipose mass[5–7]. The human body contains two main types of adipose tissue: white adipose tissue (WAT) and brown adipose tissue (BAT), each serving distinct functions. WAT primarily stores triglycerides (TG) as a lipid depot, while BAT is involved in non-shivering thermogenesis[8–10].

Notably, adipose tissues are dynamic. Under certain conditions, such as cold exposure and exercise, WAT can acquire thermogenic properties similar to BAT and convert into beige fat, an intermediate form between WAT and BAT that increases energy expenditure[11,12]. Therefore, enhancing the thermogenic capacity of WAT is a promising strategy to prevent or mitigate obesity[13].

Adipose tissue is a complex metabolic organ composed mainly of adipocytes, preadipocytes, fibroblasts, immune cells, endothelial cells, and extracellular matrix (ECM)[14]. During the progression of obesity, low-grade chronic inflammation can occur and is accompanied by progressive immune-cell infiltration into adipose tissue. These infiltrating cells undergo a series of phenotypic and functional changes that can either slow or accelerate disease progression[15,16]. Macrophages, the predominant immune cells in adipose tissue, play a central role in maintaining tissue homeostasis and regulating

immune responses. In obesity, their number, localization, and phenotype change markedly, which increases chronic low-grade inflammation in adipose tissue and exacerbates the condition[17–19]. Research indicates that the polarization of macrophages plays a crucial role in the development of obesity-associated inflammatory conditions. Furthermore, studies have established a strong correlation between macrophage function and mitochondrial activity, emphasizing its significant impact on the regulation of thermogenesis[20–25].

In this process, chemokine receptors play a crucial role as key regulatory molecules governing immune cell migration and polarization[26]. CCRL2, a chemokine receptor expressed on macrophages, contributes to immune regulation[27–31]. In previous studies of obesity, CCRL2-deficient mice show increased susceptibility to high-fat-diet–induced obesity and insulin resistance[32]. However, whether and how CCRL2 influences thermogenesis and energy metabolism by regulating the polarization state of adipose tissue-resident macrophages remains unclear.

This study reveals for the first time that CCRL2 deficiency promotes macrophage polarization toward the M1 phenotype, thereby suppressing UCP1 expression and browning capacity in subcutaneous white adipose tissue through a pathway independent of the classical β-AR-cAMP-PKA thermogenic signaling axis, ultimately leading to systemic energy metabolism dysfunction.

Results

CCRL2 knockout mice exhibit increased body weight, primarily due to alterations in adipose tissue.

Previous studies have demonstrated that deletion of the chemokine receptor CCRL2 under high-fat diet conditions exacerbates obesity and metabolic disorders in mice[32]. In this study, we observed that CCRL2 knockout mice exhibited significantly higher body weights than wild-type mice at 15 weeks of age, even when fed a standard diet (Fig. 1A). Weekly monitoring of food intake starting at week 8 revealed no significant difference in average food consumption between the two groups (Fig. 1B). Further tissue analysis demonstrated that CCRL2 knockout mice exhibited significantly increased weights of both subcutaneous and visceral white adipose tissue. Notably, their brown adipose tissue (BAT) weight was significantly reduced (Fig. 1C). These findings suggest that CCRL2 plays a role in regulating body weight and fat distribution.

CCRL2 knockout mice showed a marked reduction in heat production in subcutaneous adipose tissue under cold stimulation.

Brown adipose tissue (BAT) is essential for regulating energy homeostasis and thermogenesis[33–35]. Our study observed a notable decrease in BAT mass in CCRL2 knockout mice, prompting an investigation into CCRL2's role in thermogenesis (Fig. 1). To explore this, 8-week-old male WT and CCRL2 -/- mice were subjected into a cold challenge at 4°C for 24 hours and then analyzed two thermogenic depots: BAT and subcutaneous white adipose tissue (sWAT). In sWAT from CCRL2 knockout mice, we found a significant reduction in UCP1 protein expression(Fig. 2A). Furthermore, quantitative PCR showed substantial decreases in the thermogenic genes UCP1, PGC1α, and PRDM16 in sWAT(Fig. 2A). Interestingly, these alterations were not present in BAT(Fig. 2B). These results indicate that CCRL2 knockout in mice impairs the induction of UCP1 in sWAT in response to cold, thereby reducing the browning potential of subcutaneous fat.

In CCRL2 knockout mice, the reduction in UCP1 does not appear to correspond with the conventional thermogenic pathway.

Cold triggers the sympathetic nervous system to release norepinephrine (NE), which, upon binding to β3-AR, initiates downstream signaling pathways. This activation leads to the upregulation of genes associated thermogenesis[36,37]. To delve deeper into the effects of cold exposure, we measured two critical upstream mediators (p38 and ATF2) of UCP1 in subcutaneous adipose tissue (Fig. 3A). Interestingly, phosphorylated p38 (p-p38) levels were significantly higher in CCRL2 knockout mice, while phosphorylated ATF2 (p-ATF2) levels showed no change (Fig. 3B). Normally, UCP1 expression is positively linked to the activity of upstream p38 and ATF2[38], indicating that the observed reduction in UCP1 is not driven by the traditional p38–ATF2 thermogenic pathway. To test this hypothesis, we isolated stromal vascular fraction (SVF) cells from both wild-type and CCRL2 knockout mice, induced adipogenic differentiation, and stimulated the adipocytes with a β3-adrenergic agonist. In vitro analysis revealed no significant difference in UCP1 expression between the two genotypes. Taken together, the results suggest that the UCP1 downregulation seen in CCRL2 knockout mice after cold exposure is unlikely to arise from the conventional mitochondrial thermogenic pathway.

CCRL2 deficiency alters thermogenesis by shifting macrophages toward an M1 phenotype.

CCRL2, a chemokine receptor, has been implicated in inflammatory signaling[30,39,40]. Adipose tissue, beyond its metabolic functions, also contains a diverse population of immune cells that play vital roles in organismal thermogenesis[41]. Macrophages are central to mediating this inflammatory response[42,43]. To explore our hypothesis, we measured macrophage markers in subcutaneous adipose tissue after 24 hours of cold exposure. Initially, whole-tissue analysis revealed no significant differences in macrophage-related gene expression (Fig. 4A). Adipose tissue contains adipocytes and a stromal vascular fraction (SVF) that includes immune cells[44]. Therefore, we isolated $CD45^+$ immune cells to

quantify macrophage abundance and polarization more precisely. Flow cytometry showed a trend toward increased $CD11b^+F480^+$macrophage numbers in the subcutaneous adipose tissue of CCRL2 knockout mice and revealed a significantly larger proportion of M1-polarized macrophages ($CD11c^+CD11b^+F480^+$) than in wild-type controls (Fig. 4B-C). To investigate whether macrophages from CCRL2 knockout mice are inherently inclined towards M1 polarization, we isolated and cultured peritoneal macrophages from these mice. After stimulating them with LPS, we evaluated the expression of M1 markers. The results indicated a significant increase in M1 marker expression in macrophages from CCRL2 knockout mice, along with a notable upregulation of proteins associated with polarization-related signaling pathways (Fig. 4D). Together, these results indicate that the thermogenic phenotype of CCRL2 knockout mice is associated with macrophage polarization and the elevated presence of M1 macrophages in CCRL2 knockout mice, particularly under cold stimulation, contributes to their reduced thermogenic capacity.

Discussion

In this study, we demonstrate that CCRL2 plays an important role in energy metabolism. CCRL2, an atypical chemokine receptor expressed in immune cells, participates in diverse immune responses[27–31]. Here, we propose for the first time that CCRL2 modulates thermogenesis by shifting macrophage polarization. Because inducing browning of white adipose tissue is a promising strategy to combat obesity, these findings suggest potential new therapies for obesity and related metabolic disorders.

Our findings indicate that CCRL2 knockout mice experienced a notable increase in body weight under normal diet conditions. Additionally, their subcutaneous white adipose tissue (WAT) showed significantly reduced thermogenic capacity after cold exposure, while the thermogenic function of brown adipose tissue (BAT) remained relatively stable. This suggests that CCRL2 may influence overall energy balance by specifically modulating sWAT thermogenic activity. Mechanistic analysis revealed that CCRL2 knockout resulted in a marked decrease in UCP1 expression in subcutaneous adipose tissue, independent of the traditional adrenergic receptor (β-AR)-cAMP-PKA pathway, suggesting a non-classical regulatory mechanism. Further research demonstrated that CCRL2 affects energy metabolism by influencing macrophage polarization. In the absence of CCRL2, macrophages shifted towards the pro-inflammatory M1 phenotype, exacerbating chronic low-grade inflammation in adipose tissue and inhibiting UCP1 expression, thereby diminishing sWAT thermogenic capacity. A study on brown adipose tissue (BAT) has revealed the existence of a "mitochondrial quality control system" between brown adipocytes and macrophages. The research indicates that macrophages regulate the expression of UCP1 by removing portions of mitochondria that have undergone oxidative damage[45].This aligns with existing studies linking the inflammatory state of the adipose

tissue microenvironment to thermogenesis, with macrophage polarization playing a crucial role[46,47].

Macrophages constitute the predominant immune cell population within the stromal vascular fraction (SVF)[48]. Numerous studies have examined the relationship between macrophages and obesity[49,50]. By altering their abundance and phenotype, macrophages adopt either anti-inflammatory or proinflammatory roles, corresponding to lean or obese states.

Macrophage polarization plays a central role in obesity-associated metabolic inflammation, with chemokine receptors serving as key molecules regulating their polarization and function[51,52]. Our data reveal that CCRL2-deficient mice exhibit a significantly increased proportion of M1-type (CD11c+) macrophages in subcutaneous adipose tissue upon cold stimulation, accompanied by downregulation of key thermogenic genes such as UCP1 and PGC1α. This association suggests that CCRL2 may constitute a critical immune checkpoint, whose functional deficiency disrupts macrophage homeostasis in adipose tissue, leading to a pro-inflammatory environment that suppresses the thermogenic program of adipocytes. This mechanism shares similarities yet differs from the classical pathway dominated by the CCR2/CCL2 axis for monocyte recruitment and inflammatory amplification[51]. Previous studies indicate that CCR2 deficiency similarly alters macrophage phenotypes but may influence metabolism through distinct mechanisms[53]. This study identifies CCRL2 as a novel regulator of macrophage phenotype switching and metabolic function within the adipose tissue microenvironment, independent of CCR2. Notably, CCRL2 modulates UCP1 expression via a pathway entirely bypassing the traditional β-AR-cAMP-PKA thermogenic signaling axis. In CCRL2 knockout mice, we observed abnormally elevated p38 MAPK phosphorylation levels, yet activation of the downstream transcription factor ATF2 and its UCP1-inducing effect were decoupled. In vitro experiments further confirmed that even under direct stimulation by β3-adrenergic receptor agonists, UCP1 expression capacity remained impaired in preadipocytes derived from CCRL2 knockout mice. These findings strongly support the existence of a non-adrenergic thermoregulatory pathway initiated by “CCRL2-macrophage polarization.” This pathway may coexist with recently discovered mechanisms involving factors like PDGFcc secreted by adipose tissue-resident macrophages to regulate energy storage, collectively forming an immune-mediated adipose metabolism regulatory network independent of neural innervation[26]. Targeting CCRL2 or its downstream signaling pathways holds promise for specifically modulating energy expenditure in adipose tissue without disrupting the systemic sympathetic nervous system, providing a theoretical basis for developing anti-obesity strategies with reduced side effects.

Of course, this study also has certain limitations. First, we used a systemic CCRL2 knockout mouse model, which cannot distinguish the specific role of CCRL2 in macrophages versus other cell types (such as adipocytes or endothelial cells). Although in vitro macrophage experiments support its cell-autonomous function, the cell-specific role in adipose thermogenesis requires final confirmation using conditional macrophage knockout mice. Second, while we preliminarily revealed that CCRL2 deficiency leads to increased M1 polarization accompanied by abnormal p38 activation, the specific molecular details remain unclear. These include how CCRL2 senses microenvironmental signals, its downstream signaling pathways (e.g., whether it involves interactions with receptors such as TLR4), and the soluble factors or cell-contact mechanisms through which M1 macrophages suppress UCP1 expression in adipocytes remain to be elucidated. Finally, the potential roles of other immune cells within adipose tissue—such as T cells and neutrophils—in the metabolic network regulated by CCRL2 cannot be ruled out.

In addition, Our results are valuable from mouse studies, but species differences in physiology and immune response limit direct translation to humans. Therefore caution is required when applying these results to clinical practice and further validation with human samples.

In conclusion, this study is the first to elucidate that CCRL2 regulates macrophage polarization through a non-adrenergic pathway, affecting UCP1 expression and revealing a novel molecular mechanism by which CCRL2 regulates WAT thermogenesis independently of macrophage polarization. This discovery challenges the traditional view that thermogenesis regulation relies solely on the β-AR pathway and lays the groundwork for developing treatment strategies targeting the adipose tissue microenvironment. These efforts aim to facilitate the translation of CCRL2 research from basic discovery to clinical application, offering precise intervention strategies to address the global obesity crisis. Future research should focus on: deeply dissect the downstream signaling networks of CCRL2 within macrophages and its interactions with pathways such as p38; identify the specific effector molecules mediating thermogenesis suppression in M1 macrophages; and explore the therapeutic potential of CCRL2 functional intervention in diet-induced obesity models. These efforts will contribute to comprehensively mapping the immune system's fine-tuned regulation of energy metabolism and open new avenues for immunotherapy in metabolic diseases.

Methods

Animal studies

C57BL/6J mice were obtained from the Experimental Animal Center at Chongqing Medical University, China. Ccrl2 knockout mice were generated by Cyagen Biosciences Inc. using

TALENs microinjection into fertilized C57BL/6 mouse eggs. The mice were kept in cages on a 12-hour light/12-hour dark cycle at 22–24˚C with access to food and water, each animal experiment was conducted with animals housed in a single cage. For the cold-tolerance test, 8-week-old C57BL/6J mice on a normal diet (ND) and 8-week-old Ccrl2-deficient mice were housed with ad libitum access to food and water and maintained at 6°C, each group contained 6 to 7 mice. The number of mice mainly conforms to the commonly used quantities in the literature to ensure adequate statistical power. A total of 45 mice were included in the study including 23 WT mice and 22 ccrl2-/-mice. No animals were excluded from the analysis, mice in each group were randomly selected for experimental treatmen5. To minimize bias, the investigators performing the data analysis were blinded to the group allocation. Rectal temperature was measured using a temperature sensor. For sample collection, mice were deeply anesthetized with isoflurane (3–4% for induction, delivered in 100% oxygen). Anesthesia depth was confirmed by loss of the pedal withdrawal reflex. After confirmation of deep anesthesia, mice were euthanized by cervical dislocation. Because this was a terminal tissue-harvesting procedure and animals did not regain consciousness, no analgesic agents were administered. Samples were frozen in liquid nitrogen tanks within two hours of dissection. All the work was approved by the Ethics Committee of the Institute of Life Science, Chongqing medical university (IACUC-CQMU-2023-0156), Great care was taken to minimize animal suffering. All experiments were performed in accordance with the relevant guidelines and regulations, including the ARRIVE guidelines..

Real-time RT-PCR

Total RNA was extracted with TRIzol™ Reagent (Invitrogen) according to the manufacturer's protocol. RNA concentration and purity were quantified using a NanoDrop 2000 spectrophotometer, with A260/A280 ratios strictly verified to be between 1.8 and 2.0. Reverse transcription of 1 µg RNA was done using the RevertAid First Strand cDNA Synthesis Kit (Thermo Scientific). Quantitative PCR (qPCR) was carried out in a 10 µl reaction volume (containing 1 µl of cDNA template) with Power SYBR Green PCR Master Mix (Applied Biosystems) on an ABI Prism 7500 qPCR machine. The thermocycling conditions consisted of an initial denaturation at 95°C for 30 s, followed by 40 cycles of 95°C for 5 s and 60°C for 30 s. To verify amplicon specificity, a melt curve analysis (from 65°C to 95°C) was performed after amplification, confirming a single specific peak for each gene. A no-template control (NTC) was included in every PCR run to assess potential DNA contamination, and no amplification was detected. Amplification efficiencies for all primers were verified to be approximately 90–110%. The primers were obtained from Sangon Biotech and the sequences used in this study are listed in **Table 1**. All qPCR reactions were performed in technical triplicates. The relative expression levels of mRNAs

were calculated using the ΔΔCt method with 18s housekeeping gene as the internal control gene for normalization.

Western blot analyses

Cells were lysed in buffer containing 2% SDS and 50 mM Tris–HCl (pH 6.8). After determining protein concentrations, equal amounts of lysate were resolved by electrophoresis, transferred to membranes, and incubated with the appropriate primary antibodies. Membranes were then probed with HRP-conjugated secondary antibodies and developed. Antibodies against β-actin, UCP1, pp38 MAPK, p38 MAPK, p-ATF2, ATF2, p-p44/42 MAPK ERK, p44/42 MAPK ERK, p-NF-κB p65, and NF-κB p65 were purchased from Cell Signaling Technology Inc, USA. To optimize antibody usage and accommodate multiple protein targets, PVDF membranes were sectioned horizontally based on prestained molecular weight markers.

Isolation of stromal vascular fraction and Flow cytometry analysis

Adipose tissue was minced in PBS containing 0.075% collagenase (Sigma) and incubated at 37°C for 30 min. The digest was filtered through a 100 μm sieve. Cell suspensions were centrifuged at 400g for 5 min, and the stromal vascular fraction (SVF) formed a pellet at the tube base. The SVF pellet was resuspended in PBS with 3% BSA and treated with red blood cell lysis buffer for 3 min. After washing with 3% FBS, cells were incubated with Fc Block for 20 min at 4°C. Antibodies targeting CD45-FITC (eBioscience), F4/80-PE (BioLegend), CD11b-PerCP/Cy5.5 (BioLegend), and CD11c-APC (BioLegend) were added and incubated for an additional 20 min. Finally, cells were rinsed in PBS with 3% FBS and analyzed by flow cytometry (BD Biosciences).

Primary adipose tissue culture

Adipose tissue from ND-fed WT and CCRL2-deficient mice was excised and minced into ~ 1–2 mm fragments. The stromal vascular fraction (SVF) was isolated using standard procedures, including removal of red blood cells. Cells were rinsed twice and cultured in DMEM/*F12* medium supplemented with 10% fetal bovine serum, 1% penicillin/streptomycin (P/S), and 1% biotin.

Peritoneal Macrophage isolation, culture and polarization

Peritoneal macrophages were collected from mice after intraperitoneal injection of 5 ml of 1640 medium containing 50% FBS. Peritoneal cells were recovered by gently massaging

the abdomen for 3 minutes and then centrifuged at 1200 rpm for 5 minutes. The cell pellet was resuspended and cultured at 37°C in 5% CO2 for 1 hour; nonadherent cells were removed, adherent cells were rinsed twice with medium, and fresh medium was added. The following day, macrophages were stimulated with 10 ng/ml LPS to induce polarization. Each experimental group comprised 4 to 5 mice.

Statistical analyses

Data are expressed as mean ± standard error of the mean (SEM). For comparisons between two groups, a two-tailed Student's t-test was performed. For comparisons involving multiple groups (e.g., ratios of different tissue weights to body weight, or expression levels of multiple genes within the same tissue), one-way analysis of variance (ANOVA) was used. $P < 0.05$ was considered statistically significant. All statistical analyses were performed using GraphPad Prism 5 software.

Declarations

Acknowledgements

We sincerely thank all participants for their invaluable support and contributions to this study.

We acknowledge the use of artificial intelligence (AI) tools for language editing in the preparation of this manuscript.

Ethics approval

This work was approved by the Ethics Committee of the Institute of Life Science, Chongqing medical university (IACUC-CQMU-2023-0156).

Additional Information and Declarations

The authors declare that they have no competing interests.

Data Availability

The datasets generated and analyzed during the current study are available in the FigShare repository. Raw data for phenotypic analysis and gene expression can be accessed at https://doi.org/10.6084/m9.figshare.31397961 and the flow cytometry datasets are available at https://doi.org/10.6084/m9.figshare.31384537. All other data supporting the findings of this study are included within the manuscript and its supplementary information files.

Funding

This work was supported by the Youth Supporting Project of Northern Jiangsu People's Hospital (grant number: SBQN22021).

References

1. Magkos, F. A Hypothesis on the Historical Development of Obesity that is Not Only About Food. *Current obesity reports* **14**, 58, doi:10.1007/s13679-025-00650-y (2025).
2. Korner, J., Woods, S. C. & Woodworth, K. A. Regulation of energy homeostasis and health consequences in obesity. *The American journal of medicine* **122**, S12-18, doi:10.1016/j.amjmed.2009.01.003 (2009).
3. Charakida, M. & Finer, N. Drug treatment of obesity in cardiovascular disease. *American journal of cardiovascular drugs : drugs, devices, and other interventions* **12**, 93-104, doi:10.2165/11599000-000000000-00000 (2012).
4. Boutari, C., DeMarsilis, A. & Mantzoros, C. S. Obesity and diabetes. *Diabetes research and clinical practice* **202**, 110773, doi:10.1016/j.diabres.2023.110773 (2023).
5. Rogge, M. M. The role of impaired mitochondrial lipid oxidation in obesity. *Biological research for nursing* **10**, 356-373, doi:10.1177/1099800408329408 (2009).
6. Löffler, M. C. *et al.* Challenges in tackling energy expenditure as obesity therapy: From preclinical models to clinical application. *Molecular metabolism* **51**, 101237, doi:10.1016/j.molmet.2021.101237 (2021).
7. Hopkins, M. & Blundell, J. E. Energy balance, body composition, sedentariness and appetite regulation: pathways to obesity. *Clinical science (London, England : 1979)* **130**, 1615-1628, doi:10.1042/cs20160006 (2016).
8. Yin, N. *et al.* Fluvastatin Sodium Ameliorates Obesity through Brown Fat Activation. *International journal of molecular sciences* **20**, doi:10.3390/ijms20071622 (2019).
9. Kim, E., Lim, S. M., Kim, M. S., Yoo, S. H. & Kim, Y. Phyllodulcin, a Natural Sweetener, Regulates Obesity-Related Metabolic Changes and Fat Browning-Related Genes of Subcutaneous White Adipose Tissue in High-Fat Diet-Induced Obese Mice. *Nutrients* **9**, doi:10.3390/nu9101049 (2017).
10. Huang, C. W. *et al.* Role of n-3 Polyunsaturated Fatty Acids in Ameliorating the Obesity-Induced Metabolic Syndrome in Animal Models and Humans. *International journal of molecular sciences* **17**, doi:10.3390/ijms17101689 (2016).
11. McClung, J. A. *et al.* Heme-oxygenase and lipid mediators in obesity and associated cardiometabolic diseases: Therapeutic implications. *Pharmacology & therapeutics* **231**, 107975, doi:10.1016/j.pharmthera.2021.107975 (2022).
12. Lin, K., Dong, C., Zhao, B., Zhou, B. & Yang, L. Glucagon-like peptide-1 receptor agonist regulates fat browning by altering the gut microbiota and ceramide metabolism. *MedComm* **4**, e416, doi:10.1002/mco2.416 (2023).

13. Zou, T. *et al.* Raspberry promotes brown and beige adipocyte development in mice fed high-fat diet through activation of AMP-activated protein kinase (AMPK) α1. *The Journal of nutritional biochemistry* **55**, 157-164, doi:10.1016/j.jnutbio.2018.02.005 (2018).
14. Díaz-Chamorro, S. *et al.* Title: p38δ Regulates IL6 Expression Modulating ERK Phosphorylation in Preadipocytes. *Front Cell Dev Biol* **9**, 708844, doi:10.3389/fcell.2021.708844 (2021).
15. SantaCruz-Calvo, S. *et al.* Adaptive immune cells shape obesity-associated type 2 diabetes mellitus and less prominent comorbidities. *Nature reviews. Endocrinology* **18**, 23-42, doi:10.1038/s41574-021-00575-1 (2022).
16. Bai, Y. & Sun, Q. Macrophage recruitment in obese adipose tissue. *Obesity reviews : an official journal of the International Association for the Study of Obesity* **16**, 127-136, doi:10.1111/obr.12242 (2015).
17. Dahdah, N., Tercero-Alcázar, C., Malagón, M. M., Garcia-Roves, P. M. & Guzmán-Ruiz, R. Interrelation of adipose tissue macrophages and fibrosis in obesity. *Biochemical pharmacology* **225**, 116324, doi:10.1016/j.bcp.2024.116324 (2024).
18. Neo, W. H., Lie, A. L. M., Fadlullah, M. Z. H. & Lacaud, G. Contributions of Embryonic HSC-Independent Hematopoiesis to Organogenesis and the Adult Hematopoietic System. *Front Cell Dev Biol* **9**, 631699, doi:10.3389/fcell.2021.631699 (2021).
19. Lee-Rueckert, M. *et al.* Obesity-induced changes in cancer cells and their microenvironment: Mechanisms and therapeutic perspectives to manage dysregulated lipid metabolism. *Seminars in cancer biology* **93**, 36-51, doi:10.1016/j.semcancer.2023.05.002 (2023).
20. Kraakman, M. J., Murphy, A. J., Jandeleit-Dahm, K. & Kammoun, H. L. Macrophage polarization in obesity and type 2 diabetes: weighing down our understanding of macrophage function? *Frontiers in immunology* **5**, 470, doi:10.3389/fimmu.2014.00470 (2014).
21. Yang, Y. *et al.* Avicularin alleviates osteoporosis-induced implant loosening by attenuating macrophage M1 polarization via its inhibitory effect on the activation of NF-κB. *Biomedicine & pharmacotherapy = Biomedecine & pharmacotherapie* **158**, 114113, doi:10.1016/j.biopha.2022.114113 (2023).
22. Vassiliou, E. & Farias-Pereira, R. Impact of Lipid Metabolism on Macrophage Polarization: Implications for Inflammation and Tumor Immunity. *International journal of molecular sciences* **24**, doi:10.3390/ijms241512032 (2023).
23. Diskin, C. & Pålsson-McDermott, E. M. Metabolic Modulation in Macrophage Effector Function. *Frontiers in immunology* **9**, 270, doi:10.3389/fimmu.2018.00270 (2018).
24. Chavakis, T., Alexaki, V. I. & Ferrante, A. W., Jr. Macrophage function in adipose tissue homeostasis and metabolic inflammation. *Nature immunology* **24**, 757-766,

doi:10.1038/s41590-023-01479-0 (2023).

25. Wang, Y. N. *et al.* Slit3 secreted from M2-like macrophages increases sympathetic activity and thermogenesis in adipose tissue. *Nature metabolism* **3**, 1536-1551, doi:10.1038/s42255-021-00482-9 (2021).
26. Cox, N. *et al.* Diet-regulated production of PDGFcc by macrophages controls energy storage. *Science (New York, N.Y.)* **373**, doi:10.1126/science.abe9383 (2021).
27. Im, H. *et al.* Regulatory roles of G-protein coupled receptors in adipose tissue metabolism and their therapeutic potential. *Archives of pharmacal research* **44**, 133-145, doi:10.1007/s12272-021-01314-w (2021).
28. Mazzotti, C. *et al.* The Atypical Receptor CCRL2 (C-C Chemokine Receptor-Like 2) Does Not Act As a Decoy Receptor in Endothelial Cells. *Frontiers in immunology* **8**, 1233, doi:10.3389/fimmu.2017.01233 (2017).
29. Schioppa, T. *et al.* Molecular Basis for CCRL2 Regulation of Leukocyte Migration. *Front Cell Dev Biol* **8**, 615031, doi:10.3389/fcell.2020.615031 (2020).
30. Otero, K. *et al.* Nonredundant role of CCRL2 in lung dendritic cell trafficking. *Blood* **116**, 2942-2949, doi:10.1182/blood-2009-12-259903 (2010).
31. Galligan, C. L. *et al.* Up-regulated expression and activation of the orphan chemokine receptor, CCRL2, in rheumatoid arthritis. *Arthritis and rheumatism* **50**, 1806-1814, doi:10.1002/art.20275 (2004).
32. Xu, M. *et al.* Ccrl2 deficiency deteriorates obesity and insulin resistance through increasing adipose tissue macrophages infiltration. *Genes & diseases* **9**, 429-442, doi:10.1016/j.gendis.2020.08.009 (2022).
33. Hekmatnejad, B. & Rudnicki, M. A. Transplantation to study satellite cell heterogeneity in skeletal muscle. *Front Cell Dev Biol* **10**, 902225, doi:10.3389/fcell.2022.902225 (2022).
34. Huang, Y. *et al.* Brown adipose TRX2 deficiency activates mtDNA-NLRP3 to impair thermogenesis and protect against diet-induced insulin resistance. *The Journal of clinical investigation* **132**, doi:10.1172/jci148852 (2022).
35. Patel, B. *et al.* The Emerging Therapeutic Potential of Kisspeptin and Neurokinin B. *Endocrine reviews* **45**, 30-68, doi:10.1210/endrev/bnad023 (2024).
36. Park, J. Y. *et al.* The brown fat-specific overexpression of RBP4 improves thermoregulation and systemic metabolism by activating the canonical adrenergic signaling pathway. *Experimental & molecular medicine* **57**, 554-566, doi:10.1038/s12276-025-01411-6 (2025).
37. Rahbani, J. F. *et al.* ADRA1A-Gα(q) signalling potentiates adipocyte thermogenesis through CKB and TNAP. *Nature metabolism* **4**, 1459-1473, doi:10.1038/s42255-022-00667-w (2022).

38. Lin, J. *et al.* Hepatokine Pregnancy Zone Protein Governs the Diet-Induced Thermogenesis Through Activating Brown Adipose Tissue. *Advanced science (Weinheim, Baden-Wurttemberg, Germany)* **8**, e2101991, doi:10.1002/advs.202101991 (2021).
39. Ben Dhaou, C., Del Prete, A., Sozzani, S. & Parmentier, M. CCRL2 Modulates Physiological and Pathological Angiogenesis During Retinal Development. *Front Cell Dev Biol* **9**, 808455, doi:10.3389/fcell.2021.808455 (2021).
40. Cash, J. L., Norling, L. V. & Perretti, M. Resolution of inflammation: targeting GPCRs that interact with lipids and peptides. *Drug discovery today* **19**, 1186-1192, doi:10.1016/j.drudis.2014.06.023 (2014).
41. Trim, W. V. & Lynch, L. Immune and non-immune functions of adipose tissue leukocytes. *Nature reviews. Immunology* **22**, 371-386, doi:10.1038/s41577-021-00635-7 (2022).
42. Hasan, A. *et al.* Correlation Profile of Suppression of Tumorigenicity 2 and/or Interleukin-33 with Biomarkers in the Adipose Tissue of Individuals with Different Metabolic States. *Diabetes, metabolic syndrome and obesity : targets and therapy* **13**, 3839-3859, doi:10.2147/dmso.S251978 (2020).
43. Rahman, M. S. & Jun, H. The Adipose Tissue Macrophages Central to Adaptive Thermoregulation. *Frontiers in immunology* **13**, 884126, doi:10.3389/fimmu.2022.884126 (2022).
44. de Jong, A. J. *et al.* Lack of high BMI-related features in adipocytes and inflammatory cells in the infrapatellar fat pad (IFP). *Arthritis research & therapy* **19**, 186, doi:10.1186/s13075-017-1395-9 (2017).
45. Rosina, M. *et al.* Ejection of damaged mitochondria and their removal by macrophages ensure efficient thermogenesis in brown adipose tissue. *Cell metabolism* **34**, 533-548.e512, doi:10.1016/j.cmet.2022.02.016 (2022).
46. Xu, L. *et al.* Macrophage Polarization Mediated by Mitochondrial Dysfunction Induces Adipose Tissue Inflammation in Obesity. *International journal of molecular sciences* **23**, doi:10.3390/ijms23169252 (2022).
47. Zhang, Y., Zhang, B. & Sun, X. The molecular mechanism of macrophage-adipocyte crosstalk in maintaining energy homeostasis. *Frontiers in immunology* **15**, 1378202, doi:10.3389/fimmu.2024.1378202 (2024).
48. Lavin, Y., Mortha, A., Rahman, A. & Merad, M. Regulation of macrophage development and function in peripheral tissues. *Nature reviews. Immunology* **15**, 731-744, doi:10.1038/nri3920 (2015).
49. Li, C., Qu, L., Farragher, C., Vella, A. & Zhou, B. MicroRNA Regulated Macrophage Activation in Obesity. *Journal of translational internal medicine* **7**, 46-52, doi:10.2478/jtim-2019-0011 (2019).

50. Weisberg, S. P. *et al.* Obesity is associated with macrophage accumulation in adipose tissue. *The Journal of clinical investigation* **112**, 1796-1808, doi:10.1172/jci19246 (2003).
51. Zhang, H. *et al.* Synergistic Modulation of Inflammatory but not Metabolic Effects of High-Fat Feeding by CCR2 and CX3CR1. *Obesity (Silver Spring, Md.)* **25**, 1410-1420, doi:10.1002/oby.21900 (2017).
52. Sowers, M. L. *et al.* Multi-OMICs analysis reveals metabolic and epigenetic changes associated with macrophage polarization. *The Journal of biological chemistry* **298**, 102418, doi:10.1016/j.jbc.2022.102418 (2022).
53. Deci, M. B., Ferguson, S. W., Scatigno, S. L. & Nguyen, J. A.-O. Modulating Macrophage Polarization through CCR2 Inhibition and Multivalent Engagement.

Table

Table 1 is available in the supplementary files section

Figures

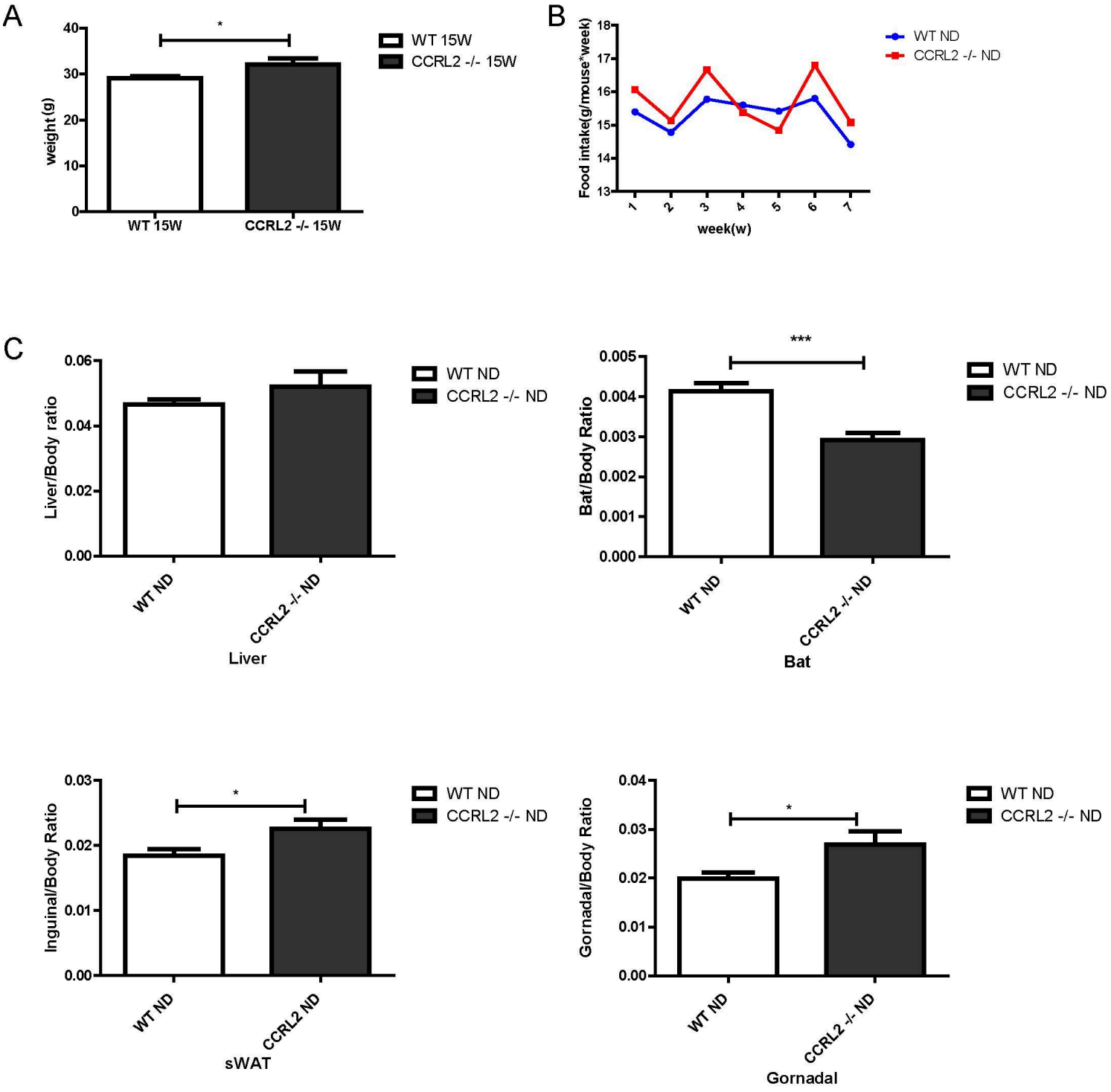


Figure 1

CCRL2 knockout mice exhibit increased body weight, primarily due to alterations in adipose tissue. (A) body weight of WT and CCRL2-/- mice fed with normal diet (n = 7). (B) Food intake of WT and CCRL2-/- mice fed with normal diet, diet was weighed weekly from the eighth week of mice(n = 7). (C) the ratio of Liver/gornadal/sWAT/Bat to body weight in WT and CCRL2-/- mice fed with normal diet(n = 7). Data are expressed as Mean ± SEM, ns = not significant, ∗P < 0.05, ∗∗P < 0.01, ∗∗∗P < 0.001.

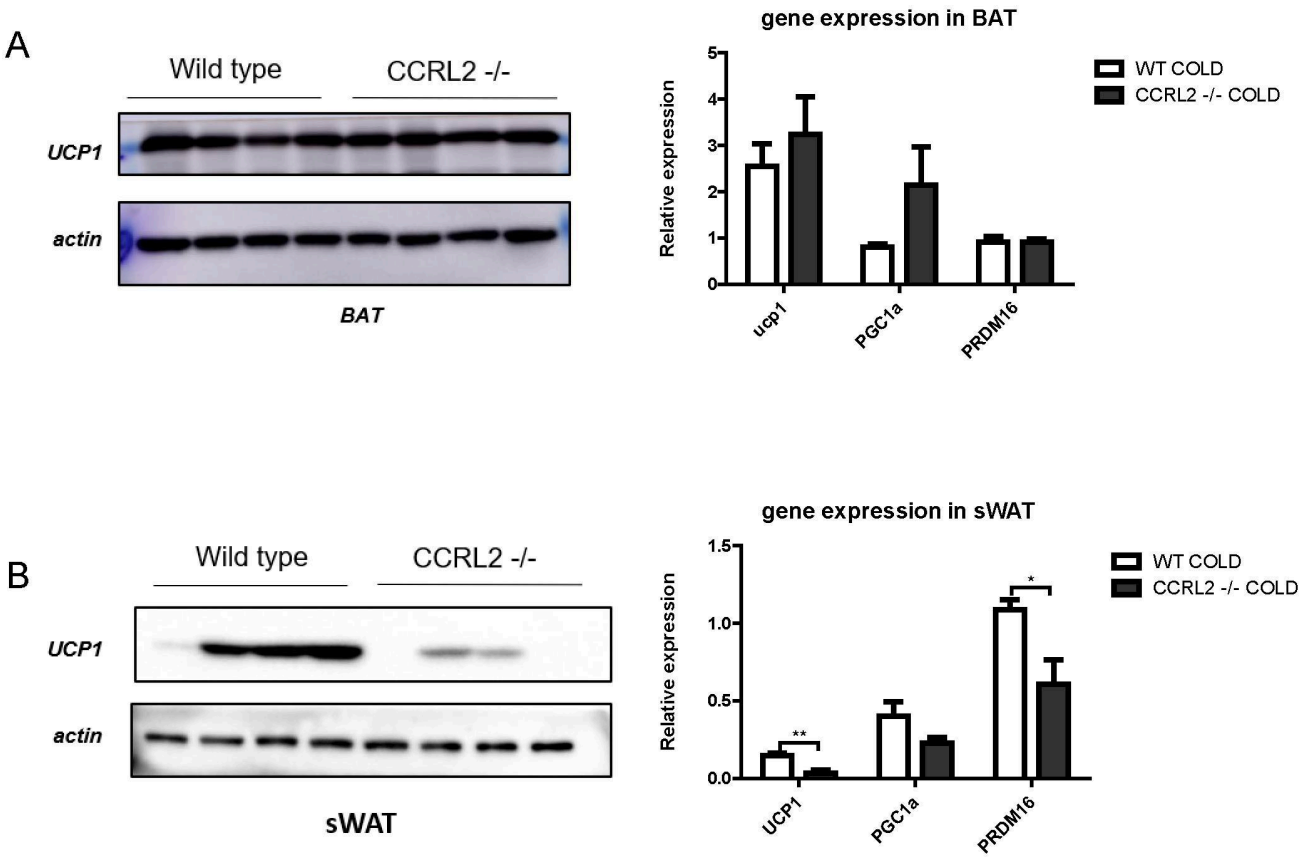


Figure 2

CCRL2 knockout mice showed a marked reduction in heat production in subcutaneous adipose tissue under cold stimulation. (A) Western blot analysis of UCP1 protein in the BAT (n = 4). (B) mRNA levels of thermogenic genes including UCP1, PGC1α and PRDM16 in the BAT(n = 6). (C) Western blot analysis of UCP1 protein in the sWAT (n = 4). (D) mRNA levels of thermogenic genes including UCP1, PGC1α and PRDM16 in the sWAT(n = 5). Data are expressed as Mean ± SEM, ns = not significant, ∗P < 0.05, ∗∗P < 0.01, ∗∗∗P < 0.001.

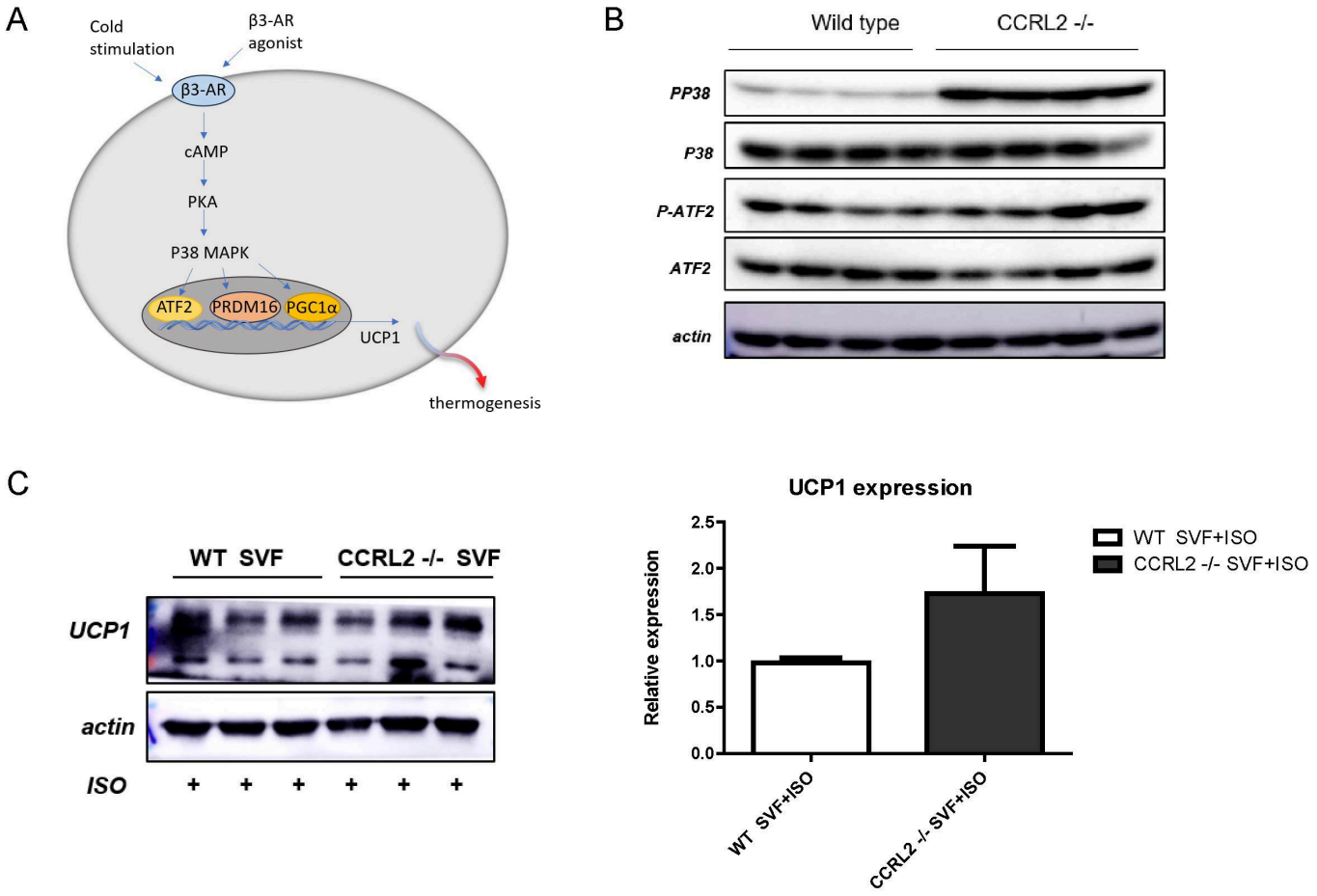


Figure 3

In CCRL2 knockout mice, the reduction in UCP1 does not appear to correspond with the conventional thermogenic pathway. (A) Schematic diagram of hypothermia/adrenergic agonist activation of the β -AR-CAMP-PKA signaling axis in mouse adipose tissue. (B) Western blot analysis of PP38/P38, PATF2/ATF2, actin protein in the sWAT (n = 4). (C) Western blot analysis of UCP1 protein in the adipogenic cells induced by SVF derived subcutaneously in mice (n = 3, left). mRNA levels of UCP1 in the adipogenic cells induced by SVF derived subcutaneously in mice (n = 3, right). Data are expressed as Mean ± SEM, ns = not significant, ∗P < 0.05, ∗∗P < 0.01, ∗∗∗P < 0.001.

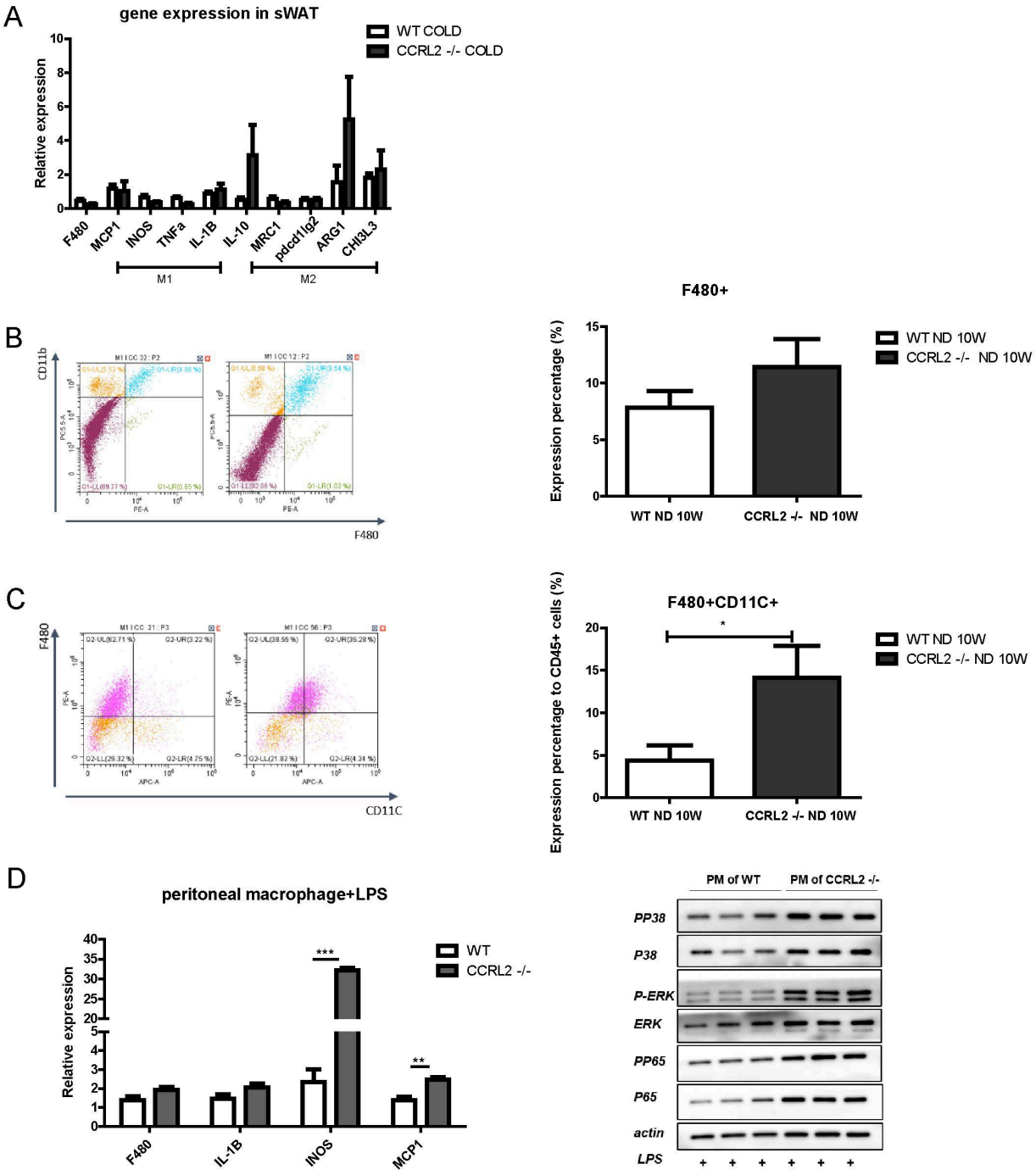


Figure 4

CCRL2 deficiency alters thermogenesis by shifting macrophages toward an M1 phenotype. (A) ATMs associated inflammation markers in sWAT (n = 6). (B) FCM analysis of proportion of macrophages in sWAT in mice fed with normal diet (n = 7). (C) FCM analysis of proportion of CD11c+macrophages in sWAT in mice fed with normal diet (n = 7). (D) mRNA levels of M1 macrophages associated genes of LPS stimulated peritoneal

macrophages from WT and ccrl2−/− mice(n = 3, left). Western Blot of M1 macrophages associated protein of LPS stimulated peritoneal macrophages from WT and ccrl2−/− mice(n = 3, right). Data are expressed as Mean ± SEM, ∗P < 0.05, ∗∗P < 0.01, ∗∗∗P < 0.001.

Supplementary Files

This is a list of supplementary files associated with this preprint. Click to download.

- table1Primer.xlsx
- reassembledpiecescoldBATF2A.jpg
- reassembledpiecescoldsWATF2B.jpg
- reassembledpiecesSWATF3B.jpg
- reassembledpiecessvfisoF3C.jpg
- reassembledpiecesPMF4D.jpg